JOURNAL OF GEOPHYSICAL RESEARCH, VOL. 115, E04008, doi:10.1029/2009JE003327, 2010

Evaluation of the orogenic belt hypothesis for the formation of the Thaumasia Highlands, Mars

Amanda L. Nahm[1,2] and Richard A. Schultz[1]

Received 6 April 2009; revised 2 November 2009; accepted 18 November 2009; published 22 April 2010.

[1] Thrust faults along the southern margin of the Thaumasia Highlands, Mars, comprise a set of discrete subparallel south verging structures. Previous work proposed that the faults collectively define a narrow Earth-like orogenic belt composed of a deformed lithospheric section translating southward through Tharsis above a regional décollement. This hypothesis is tested here by comparing topographic slopes across the Thaumasia Highlands to the values required by thrust faulting in a critical taper wedge setting. In general, topographic slopes across the Thaumasia Highlands, 0.418–1.017°, are too shallow for the Martian lithosphere to have deformed as a critical taper wedge, assuming reasonable values for pore fluid pressure ratios and frictional strengths of the wedge material and putative décollement. Combined with the absence of a mechanism to provide the necessary values of horizontal shortening (hundreds of km), nearly lithostatic pore fluid pressure ratios, and nearly frictionless décollements over regional scales on Mars that would be necessary for lithospheric translation as a wedge, the results are consistent with thrust fault deformation across Mars that is not integrated at depth into subhorizontal structures, but which function instead as discrete structures.

Citation: Nahm, A. L., and R. A. Schultz (2010), Evaluation of the orogenic belt hypothesis for the formation of the Thaumasia Highlands, Mars, *J. Geophys. Res.*, *115*, E04008, doi:10.1029/2009JE003327.

1. Introduction

[2] The formation of the Thaumasia Highlands on Mars (Figure 1) has been an important and unresolved problem for over 30 years while becoming increasingly recognized as critical to the understanding of early Mars [*Williams et al.*, 2008; *Andrews-Hanna*, 2009]. Several hypotheses have been proposed for their formation, such as crustal uplift through intrusion of magma at depth [*Frey*, 1979; *Dohm and Tanaka*, 1999; *Dohm et al.*, 2001], an orogenic belt produced by an ancient period of plate tectonics or large-scale lateral crustal mobility [*Courtillot et al.*, 1975; *Anguita et al.*, 2001, 2006], downslope movement of Thaumasia as a block due to gravitational collapse of a volcanic edifice [*Wise et al.*, 1979, *Webb and Head*, 2002, *Borraccini et al.*, 2007] or continental-scale salt tectonics [*Montgomery et al.*, 2009], and a flexural response due to a volcanic load [*Williams et al.*, 2008]. The Thaumasia Highlands have remnant crustal magnetization [*Connerney et al.*, 2005; *Lillis et al.*, 2008a, 2008b], which suggests that the crust beneath the Thaumasia Highlands is Noachian since the cessation of crustal magnetization (and therefore, the core dynamo) occurred ~4 Ga [*Arkani-Hamed*, 2004; *Lillis et al.*, 2008a, 2008b] and occurred quickly, likely taking less than 20 Ma [*Lillis et al.*, 2008a]. Since crustal magnetization of the Thaumasia Highlands is still present, this area was not completely thermally demagnetized by long-lived Tharsis-related magmatism or underplating after the cessation of the dynamo, as is the case for the majority of Tharsis [*Johnson and Phillips*, 2005; *Lillis et al.*, 2009]. The presence of this magnetization effectively rules out the formation of the Thaumasia Highlands by crustal uplift produced by intrusion of magma in the postdynamo era (i.e., late Noachian or younger) since the magma would be a significant heat source and would thermally demagnetize the crust surrounding the intrusion [*Lillis et al.*, 2009]. The Thaumasia region has the thickest crust on Mars; in Syria Planum, the crustal thickness is 92 km and the crust under the Thaumasia Highlands is ~80 km thick [*Zuber et al.*, 2000]. A negative free-air gravity anomaly is present immediately exterior to the margin of the Thaumasia Highlands from Claritas Fossae to the west, south along the Thaumasia Highlands, east along the Coprates Rise, and terminates at Valles Marineris [*Zuber et al.*, 2000; *Williams et al.*, 2008]. This anomaly may represent a density contrast in the crust or mantle and has been interpreted to be the result of the burial of a flexural moat and a low-density crustal root that was created by the volcanic load on the surface that caused the formation of the Thaumasia Plateau [*Williams et al.*, 2008].

[3] The formation of the Thaumasia Highlands is a key question in Mars science because Thaumasia constitutes a significant and early portion of the Tharsis rise [*Frey*, 1979; *Plescia and Saunders*, 1982; *Scott and Tanaka*, 1986; *Tanaka et al.*, 1991; *Dohm and Tanaka*, 1999; *Anderson et*

[1]Geomechanics-Rock Fracture Group, Department of Geological Sciences and Engineering, University of Nevada, Reno, Nevada, USA.
[2]Now at Center for Lunar Science and Exploration, USRA Lunar and Planetary Institute, Houston, Texas, USA.

0148-0227/10/2009JE003327

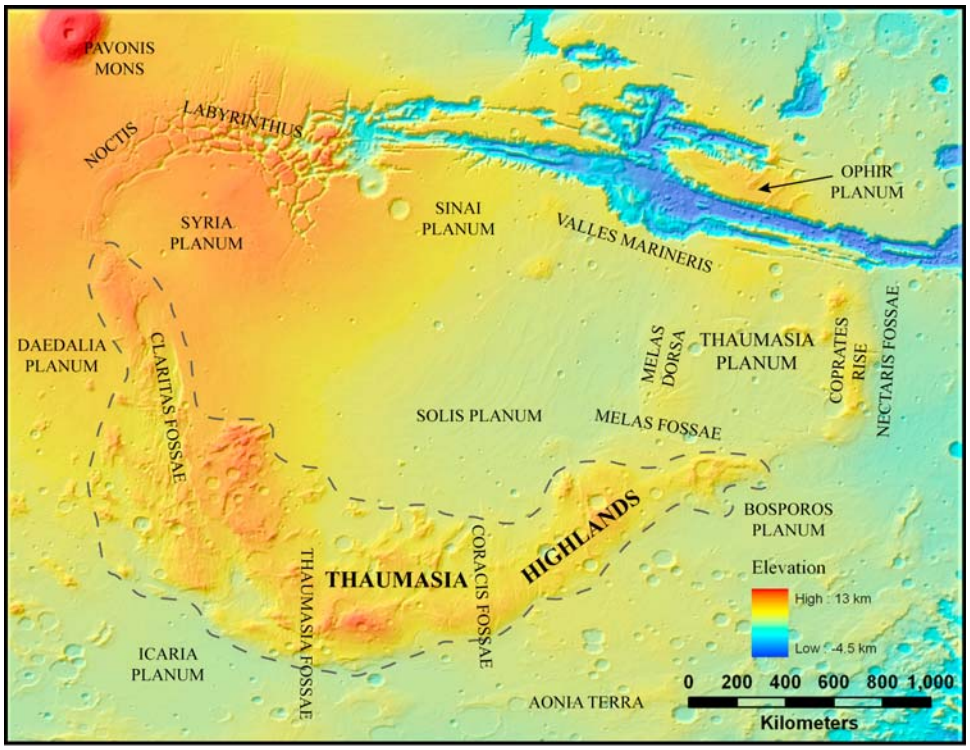

Figure 1. Index map showing the Thaumasia region, Mars. Key locations are labeled. Location of the Thaumasia Highlands outlined by dotted line. The Thaumasia Plateau encompasses the Thaumasia Highlands and the plains between them and Valles Marineris. Base image is MOLA topography. Elevation scale shown in bottom right portion of image. The northeast corner is located at 1°4′50″N, 51°6′56″W and the southwest corner is located at 48°57′42″S, 116°43′43″W.

al., 2001; *Williams et al.*, 2008], and understanding its history contributes to the understanding of the volcanotectonic history of the Tharsis region itself [*Dohm and Tanaka*, 1999; *Andrews-Hanna*, 2009]. Understanding the evolution of Tharsis is critical to understanding the tectonic and geologic evolution of Mars [*Anderson et al.*, 2001], given its importance to regional and global deformation of the planet [*Phillips et al.*, 2001; *Golombek and Phillips*, 2010]. Tharsis is the largest volcanotectonic province on Mars and has been active throughout Martian history [*Dohm and Tanaka*, 1999; *Anderson et al.*, 2001; *Phillips et al.*, 2001; *Solomon et al.*, 2005; *Golombek and Phillips*, 2010].

[4] Thrust faults on Mars are considered to have formed from a combination of local, regional, or global stress fields that originated in several ways: (1) the Tharsis load, which is thought to have produced concentric wrinkle ridges related in part to membrane stresses in the lithosphere [*Wise et al.*, 1979; *Watters and Maxwell*, 1986; *Banerdt et al.*, 1992; *Phillips et al.*, 2001], (2) impact craters, which localize strain to produce wrinkle ridges along buried crater rims or wrinkle ridges which form as a response to internal contraction of volcanics that infill the craters [*Chicarro et al.*, 1985; *Allemand and Thomas,* 1995; *Thomson and Head*, 2001; *Head et al.*, 2002], (3) flexure caused by erosion of the dichotomy boundary, which induced compression along it in northern Terra Cimmeria and northern Arabia Terra [*Watters*, 2003; *Watters and McGovern*, 2006; *Watters et al.*, 2007], or (4) global contraction, which would create an elevated background compressive stress across the entire planet [*Solomon and Chaiken*, 1976; *Tanaka et al.*, 1991; *Banerdt et al.*, 1992; *Watters*, 1993; *Mangold et al.*, 2000; *Watters and McGovern*, 2006; *Andrews-Hanna et al.*, 2008; *Golombek and Phillips*, 2010].

[5] In this study we evaluate the orogenic belt hypothesis for the formation of the Thaumasia Highlands by using critical taper wedge mechanics (CTWM). This approach has been used to understand the formation and evolution of orogenic belts on Earth and Venus and is applied to Martian tectonics in this paper. CTWM describes the behavior of crustal sections at the planetary surface that are subjected to sufficiently large horizontal compression. The compression produces horizontal shortening in the crust and, over time and given appropriate conditions, an orogenic belt is formed. We investigate the ranges of values for key physical parameters necessary for formation of an orogenic belt on Mars assuming CTWM and compare them to typical values for terrestrial orogenic wedges.

2. Thaumasia Region

[6] The Thaumasia region is a major volcanotectonic province that lies at the southern edge of Tharsis. It includes the Thaumasia Plateau, with high interior plains partially bounded by an arcuate region of higher topography, known as the Thaumasia Highlands (Figure 1) [*Dohm and Tanaka*, 1999; *Williams et al.*, 2008]. The Thaumasia Highlands are the dominant physiographic feature of the plateau, extending nearly 2900 km in length and rising as much as 4 km above

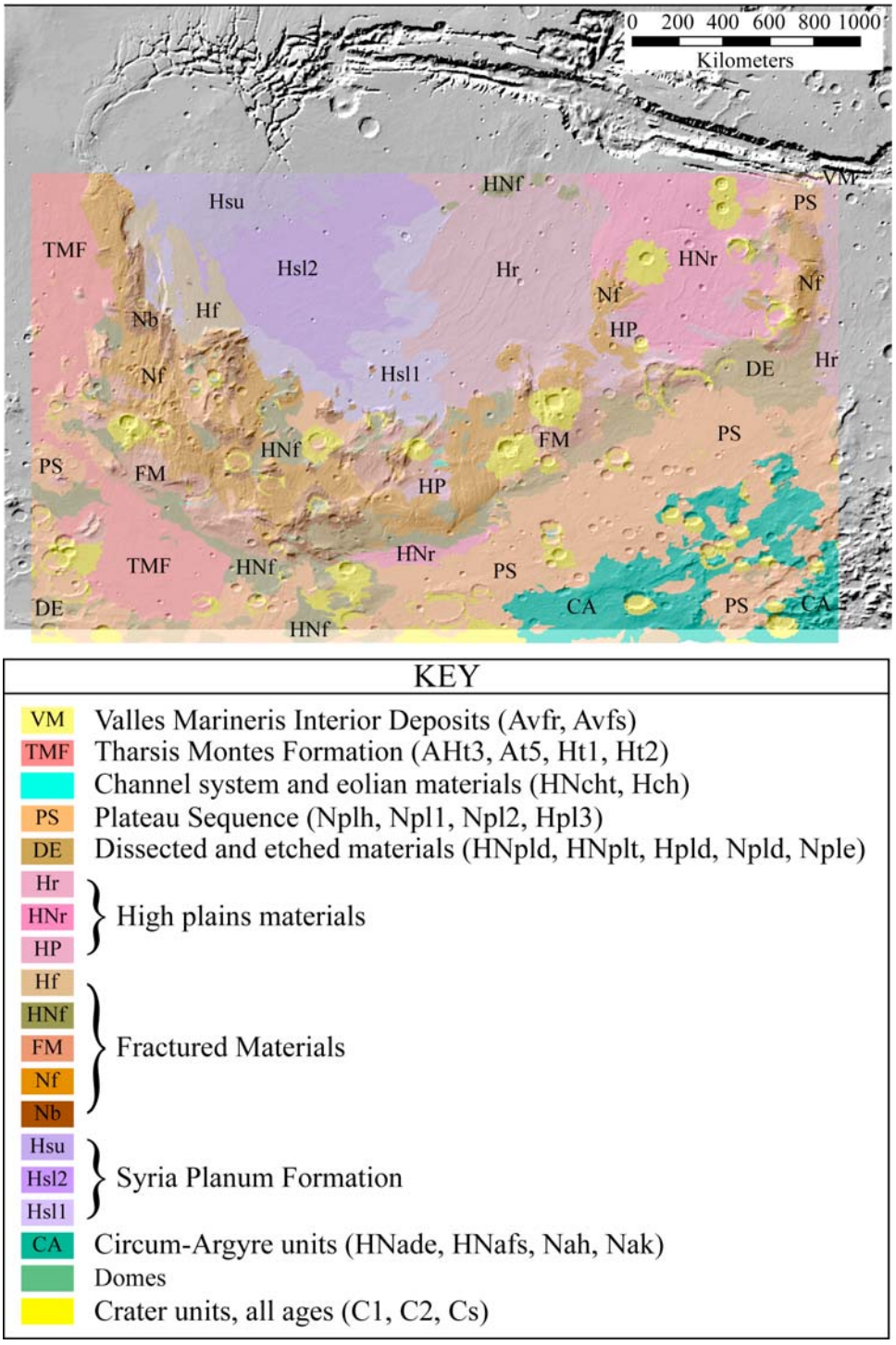

Figure 2. Abridged geologic map of the Thaumasia region, after *Dohm et al.* [2001]. Unit HP consists of HNt, HNu; unit FM consists of NFd, HNfu.

the surrounding terrain [*Dohm and Tanaka*, 1999; *Anguita et al.*, 2006]. Valles Marineris crosscuts the Thaumasia Plateau to the north, while Claritas Fossae and the Coprates Rise mark its western and eastern boundaries, respectively. Syria Planum, a volcanotectonic center active from Noachian to early Amazonian times [*Tanaka and Davis*, 1988; *Tanaka et al.*, 1996; *Dohm and Tanaka*, 1999], is located in the northwestern portion of the plateau. Noctis Labyrinthus is located along the northern edge of Syria Planum. Claritas, Thaumasia, Coracis, Melas, and Nectaris Fossae are graben sets that strike NNW and crosscut the plateau from west to east, respectively. *Schultz and Tanaka* [1994] and *Okubo and Schultz* [2004] suggest that the plateau is part of a south Tharsis ridge belt, which is defined in part by large thrust faults and anticlinal folds.

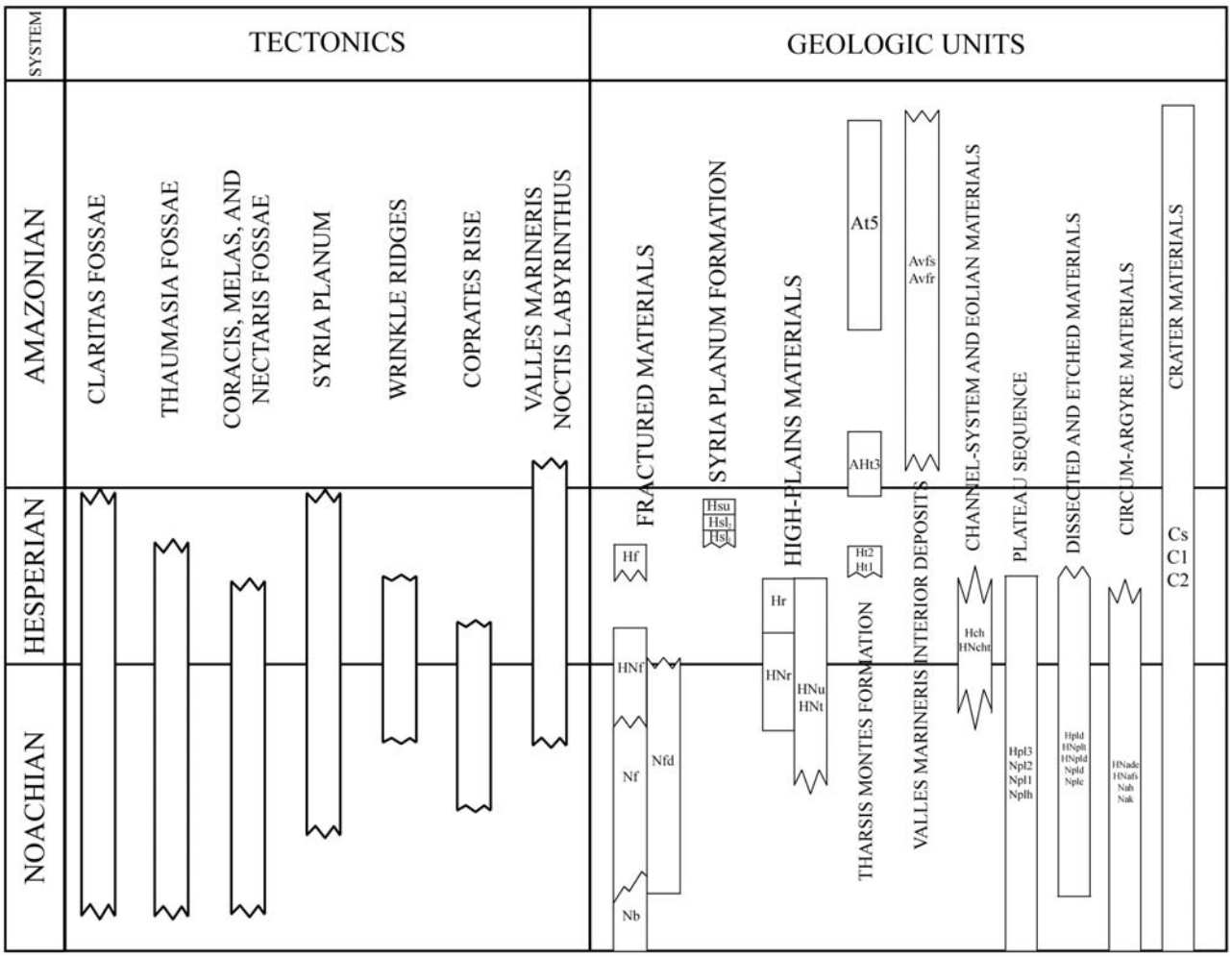

Figure 3. Chart showing stages of geologic activity, tectonics, and ages of relevant geologic units for the Thaumasia Plateau region. Boundary ages for Noachian (3.5–3.7 Ga) and Hesperian (2.9–3.3 Ga) from *Hartmann and Neukum* [2001]. Modified from *Dohm and Tanaka* [1999] and *Dohm et al.* [2001].

[7] The Thaumasia Highlands have been mapped as mostly Noachian basement and Noachian and Hesperian fractured units (units Nb, Nf, Hf, and HNf; Figure 2), with the remainder of the Thaumasia Highlands mapped as local Noachian and Hesperian units and crater materials [*Scott and Tanaka*, 1986; *Dohm and Tanaka*, 1999; *Dohm et al.*, 2001]. By using crater counting, the age of the Thaumasia Highlands has been estimated to be between ~4 Ga and ~3 Ga [*Anguita et al.*, 2006]. More precisely, the timing of the formation of the Thaumasia Highlands has been placed earlier, in the early Noachian, by study of the stratigraphic relationships of the units that comprise and embay the Thaumasia Highlands [*Williams et al.*, 2008], as well as the presence of remnant magnetization [*Connerney et al.*, 2005; *Lillis et al.*, 2008a, 2008b].

[8] The plains surrounding the Thaumasia Highlands consist of Noachian cratered materials (unit PS; Figure 2) to the south, Upper Hesperian ridged plains (unit Hr; Figure 2) to the east, and lower Amazonian lobate lava flows (unit TMF; Figure 2) emanating from Daedalia Planum to the west [*Dohm and Tanaka*, 1999; *Dohm et al.*, 2001]. The interior plains of the Thaumasia Plateau are primarily Hesperian lava flows (units Hsu: Syria Planum, Hsl_2: Solis Planum, Hsl_1 and Hr: Sinai Planum, HNr: Thaumasia Planum; Figure 2); in eastern Sinai Planum and Thaumasia Planum, these lava flows have been deformed by wrinkle ridges [*Dohm et al.*, 2001].

[9] The tectonic histories of Mars and Thaumasia are recorded by the distribution and ages of fault systems [*Dohm and Tanaka*, 1999; *Anderson et al.*, 2001]. Of the ~15,000 faults mapped over the planet [*Knapmeyer et al.*, 2006, 2008], the majority occur in and around Tharsis. Tectonic activity in Thaumasia occurred early in the development of Tharsis [*Frey*, 1979; *Plescia and Saunders*, 1982; *Tanaka et al.*, 1991; *Dohm and Tanaka*, 1999; *Anderson et al.*, 2001], peaked during the Noachian, and declined during the Hesperian through the Amazonian (Figure 3) [*Dohm and Tanaka*, 1999; *Anderson et al.*, 2001].

[10] The Thaumasia Highlands are cut by several sets of Tharsis radial graben [*Dohm and Tanaka*, 1999] (Figure 1), including Thaumasia, Claritas, Coracis, Melas, and Nectaris Fossae [*Dohm and Tanaka*, 1999]. The margin is defined locally by south verging thrust faults (either in the form of wrinkle ridges or lobate scarps) [*Plescia et al.*, 1980;

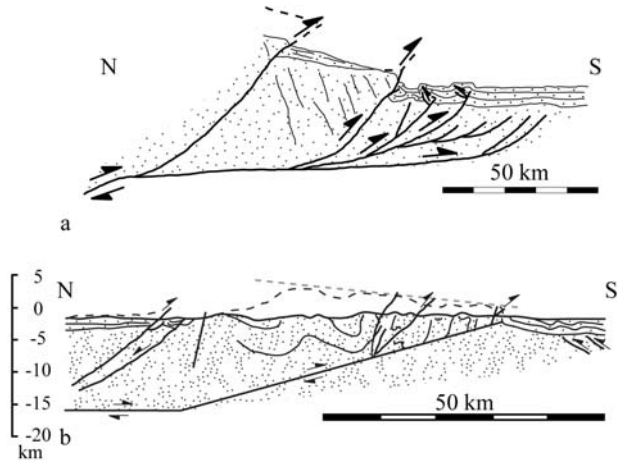

Figure 4. Comparison of (a) a schematic southern Thaumasia Highlands cross section with (b) one of the Alpine Cantabrian belt in northern Spain. Redrawn after *Alonso and Pulgar* [2004] and *Anguita et al.* [2006].

Saunders et al., 1980; *Watters*, 1993; *Dohm and Tanaka*, 1999] that are also crosscut by graben sets, such as Thaumasia Fossae [*McGill*, 1979], that may also be primarily Noachian in age [*Tanaka et al.*, 1991; *Anderson et al.*, 2001]. late Noachian–early Hesperian compression produced wrinkles ridges in Sinai and Thaumasia Plana and in eastern Coprates [*Dohm and Tanaka*, 1999].

3. Formation Models

[11] The formation of the Thaumasia Highlands topography (Figure 1) is suggested to have occurred as the flexural response to loading of the lithosphere [*Williams et al.*, 2008]. By idealizing the Thaumasia Plateau as a thick disk-shaped volcanic load, *Williams et al.* [2008] demonstrated how the load could have caused flexure of the underlying lithosphere as well as rotation of the plateau margins toward the plateau interior during the early Hesperian. The Thaumasia Highlands from Claritas Fossae [*Hauber and Kronberg*, 2005] in the west and southwest to the Coprates Rise in the east thus would represent the uplifted flexural margin of the load. A corresponding flexural moat then formed immediately exterior to the plateau margin [*Williams et al.*, 2008] (i.e., exterior to the Thaumasia Highlands) as evidenced by a negative free-air anomaly that lies immediately exterior to the Thaumasia Highlands margin [*Zuber et al.*, 2000; *Williams et al.*, 2008]. Erosion of the Thaumasia Highlands during the late Noachian–early Hesperian has partially filled the moat with sediment, along with creating valley networks along or near the crest of the Thaumasia Highlands [*Ansan and Mangold*, 2006; *Mangold and Ansan*, 2006]. Based on the flexure model [*Williams et al.*, 2008], near-surface horizontal compression would primarily occur interior to the plateau margin. However, lobate scarps, wrinkle ridges, and other compressional structures were formed during Noachian to early Hesperian time (4 Ga – 3.5 Ga) [*Hartmann and Neukum*, 2001] along the southern and eastern margins of the Thaumasia Highlands [*Schultz and Tanaka*, 1994; *Dohm and Tanaka*, 1999], indicating that the thrust faulting generally postdates the flexural topography.

[12] Several hypotheses have been suggested for the deformation and growth of the Thaumasia Highlands. These formation models were largely developed before the publication of *Williams et al.*'s [2008] key paper. The first hypothesis postulates that the Thaumasia Plateau moved downslope from Syria Planum as a single coherent lithospheric block [*Anguita et al.*, 2001; *Webb and Head*, 2002; *Borraccini et al.*, 2007] along a weak horizon (or décollement) [*Montgomery et al.*, 2009], either by gravitational collapse of some large volcanic edifice [*Webb and Head*, 2002, *Borraccini et al.*, 2007], gravity flow and sliding of near-surface lithosphere off Tharsis [*Wise et al.*, 1979], or as a result of gravitationally driven continental-scale salt tectonics [*Montgomery et al.*, 2009]. During the conjectural southeastward movement of the Thaumasia Plateau lithospheric block, proto-Valles Marineris would have functioned as a left lateral strike-slip zone [*Borraccini et al.*, 2007], and Claritas Fossae as a right lateral strike-slip zone [*Wise et al.*, 1979; *Webb and Head*, 2002], in contradiction to the evidence for predominantly normal faulting in these areas [e.g., *Tanaka et al.*, 1991; *Banerdt et al.*, 1992; *Lucchitta et al.*, 1992; *Hauber and Kronberg*, 2005]. Alternately, southeastward motion of the Thaumasia Plateau was conjectured to have produced right lateral strike-slip motion along proto-Valles Marineris [as suggested by *Webb and Head*, 2002; *Borraccini et al.*, 2007], for which there is also no evidence [e.g., *Schultz*, 1991, 1998; *Mège and Masson*, 1996]. More recently, *Montgomery et al.* [2009] speculated that the Coprates Rise and the Thaumasia Highlands mark the stratigraphic limit of a regional-scale detachment below the Thaumasia Plateau or else represent a "deformation front" where gravity spreading of the Thaumasia Plateau ceased. Their scenario also requires strike-slip motion along both Valles Marineris and Claritas Fossae, as well as a sufficiently massive volcanic center, adequate heat input (presumably from magma intrusion), a significant topographic gradient, and a sufficiently weak basal layer. Although full investigation of this megalandslide hypothesis exceeds the scope of this paper, its implications for orogenic belts in the Thaumasia Highlands will be evaluated.

[13] The second more focused hypothesis, tested in this paper, postulates that the Thaumasia Highlands represent the remnants of an ancient orogenic belt, which formed during a period of related large-scale lithospheric deformation, as could be produced during a period of ancient plate tectonics or other episode of tectonic deformation [*Courtillot et al.*, 1975, *Anguita et al.*, 2001, 2006]. The Thaumasia–Aonia Orogen, as it has been called, is suggested to have occurred sometime between Noachian and early Hesperian times [*Anguita et al.*, 2006]. This hypothesis suggests a multistage sequence of compressional deformation. In particular, it suggests that a north–south directed compression caused shortening of Thaumasia along this direction, triggering southward directed thrusting along its southern margin. *Anguita et al.* [2006] explicitly compared the Thaumasia Highlands to orogenic belts on Earth, such as the Alpine Cantabrian belt in the Pyrenees of northern Spain (Figure 4), motivating their hypothesis that the Thaumasia Highlands formed as an orogenic fold-and-thrust belt.

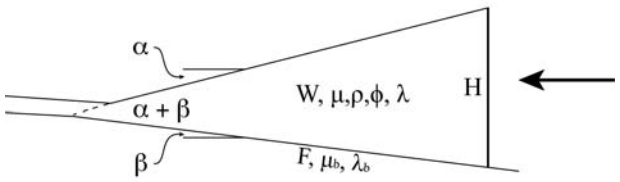

Figure 5. Schematic geometry of a critical taper orogenic wedge. Arrow on right represents horizontal compression. Variables are discussed in text. After *Dahlen* [1990] and *Suppe* [2007].

[14] Although critical taper orogenic wedges commonly occur on Earth near subduction zones and therefore in association with plate tectonics, they represent a general process of crustal deformation that results in thrust nappes and overthrust terranes [e.g., *Price and Cosgrove*, 1990], since they also are known to occur on Earth in nonplate tectonic settings [*Suppe and Connors*, 1992]. For example, fold-and-thrust belts are found at the base of sliding continental margins and deltas (offshore Texas) [*Worrall and Snelson*, 1989; *Mount*, 1989; *Mount et al.*, 1990] and on the flanks of large volcanoes on Earth and Mars [*Borgia et al.*, 1990; *Morgan and McGovern*, 2005]. The plate tectonics hypothesis for the formation of the dichotomy boundary [*Sleep*, 1994] or the crust in Meridiani Terra [*Connerney et al.*, 2005] is not widely accepted as a plausible model [*Pruis and Tanaka*, 1995] given the lack of evidence for subduction zones or other diagnostic structures [*Courtillot et al.*, 1975]. The driving forces for critical taper orogenic wedges need not involve plate tectonics or subduction, as gravity-induced sliding, for example, also requires that the upper plate above the décollement acquire the wedge geometry before sliding can occur [*Davis et al.*, 1983; *Price and Cosgrove*, 1990]. By implication, the Thaumasia Highlands formation models as proposed by *Anguita et al.* [2006] and *Montgomery et al.* [2009] require critical taper wedge mechanics, regardless of the driving mechanism for their movement. In this paper, the orogenic belt hypothesis for the formation of the Thaumasia Highlands is tested using critical taper wedge mechanics.

4. Approach: Critical Taper Wedge Mechanics

[15] Critical taper wedge mechanics (CTWM) has been used to describe the formation and development of fold-and-thrust belts such as the Central Mountains of Taiwan and the Himalaya orogens on the Earth [*Davis et al.*, 1983; *Dahlen et al.*, 1984; *Dahlen*, 1990; *Suppe*, 2007] and the Artemis Chasma, Maxwell Montes, and Uorsar Rupes fold-and-thrust belts on Venus [*Suppe and Connors*, 1992; *Williams et al.*, 1994], a planet that lacks plate tectonics. When a lithospheric section is subjected to a sufficiently large horizontal compression (defined as that producing ~150–200 km of total horizontal shortening [*Nemčok et al.*, 2005, pp. 26–45] versus any later postdécollement shortening [*Alonso et al.*, 1996]), it first deforms internally, forming nested and duplexing low-angle thrust faults (less than 30°) [e.g., *Davis et al.*, 1983] verging in the direction of transport [*Mitra and Sussman*, 1997] as seen in many orogenic belts on the Earth including the Appalachians, Himalaya, and Central Mountains [*Davis et al.*, 1983; *Suppe*, 2007]. In order to accommodate still larger amounts of shortening, the crustal section adjusts its cross-sectional geometry, thinning in the direction of transport and forming a wedge shape until a critical taper is achieved [*Chapple*, 1978] that balances the weight and frictional resistance on the newly formed décollement that defines its base [*Davis et al.*, 1983]. As deformation progresses, the wedge thickens and the point of active deformation moves away from the thickest part of the wedge (toward the toe) until the critical taper is reached [*Davis et al.*, 1983]. The wedge then slides stably along the décollement, without any additional internal deformation, and grows self-similarly as material is added at the toe [*Davis et al.*, 1983; *Davis and Engelder*, 1985].

[16] The presence of salt in compressional tectonic settings alters the way in which critical taper wedges deform. Salt (primarily halite and minimally, other evaporites) is 1–2 orders of magnitude weaker (given by its lower yield stress) than other common rock types (such as basalt) [*Davis and Engelder*, 1985], and for this reason it commonly forms décollements in regions where sufficiently large quantities are present (e.g., the Appalachian Plateau, the Jura Mountains of the Alps, the Atlas Mountains, the Zagros, the Pyrenees, and the Salt Range in Pakistan) [*Davis and Engelder*, 1985; *Costa and Vendeville*, 2002]. Critical taper wedges that have décollements in salt are characterized by their very shallow taper (~1°) and much larger upslope width than ones that do not involve a basal salt layer [*Davis and Engelder*, 1985; *Costa and Vendeville*, 2002]. In terrestrial fold-and-thrust belts without underlying salt, thrust faults tend to verge consistently toward the toe of the wedge [*Davis and Engelder*, 1985; *Mitra and Sussman*, 1997], whereas in salt décollement fold-and-thrust belts, a preferred thrust fault vergence direction [*Davis and Engelder*, 1985; *Costa and Vendeville*, 2002] or duplexing thrust faults are not present [*Costa and Vendeville*, 2002]. Because salt deforms by ductile flow at the temperature and pressure conditions found at shallow depths on Earth, salt-cored anticlines are produced as deformation progresses, as seen for example in the Franklin Mountains of northwestern Canada [*Davis and Engelder*, 1985; *Costa and Vendeville*, 2002].

[17] CTWM can be described using equations that characterize the physical properties and geometry of the wedge. The surface slope (α, in radians) of a mechanically homogeneous wedge is related to the dip angle of the décollement (β, in radians; see Figure 5 and Table 1) by [*Suppe*, 2007]:

$$\beta = \frac{F - \alpha\left[\left(1 - \left(\rho_f/\rho\right)\right) + W\right]}{W} \tag{1}$$

$$F = \mu_b(1 - \lambda) + S_b/\rho g H \tag{2}$$

$$W = 2(1 - \lambda)[\sin\phi/(1 - \sin\phi)] + C/\rho g H \tag{3}$$

where F is the nondimensional décollement strength, W is the nondimensional wedge strength, ρ_f is the density of the overlying fluid (in this case, the density of the Martian atmosphere), ρ is the average density of the wedge material, μ_b is the coefficient of friction of a décollement, λ is the pore fluid pressure ratio in the wedge ($\lambda = P_f/\rho g z$, where P_f is the

Table 1. Definition of Variables and Values Used in the Calculations

Parameter	Description	Value(s)	Source
		Wedge	
μ	Wedge friction coefficient	0.1, 0.2, 0.4, 0.6, 0.85, 1.0	*Davis et al.* [1983]; *Lin and Stein* [2004]; *Toda et al.* [2005]
Φ	Angle of internal friction for the wedge	5.7°, 11.5°, 21.8°, 30°, 40.4°, 45°	$\Phi = \tan^{-1} \mu$
ρ	Density of the wedge material	3055 kg m^{-3}	*Williams et al.* [2008]
λ	Pore fluid pressure ratio in the wedge	0 – 0.9, in 0.2 increments	*Hubbert and Rubey* [1959]
α	Surface slope	Measured; See Figure 6	
C	Wedge cohesion	25 MPa	*Suppe and Connors* [1992]
W	Wedge strength		
H	Wedge thickness	Calculated; See Figure 6	
		Décollement	
S_b	Décollement cohesion	25 MPa	*Suppe and Connors* [1992]
μ_b	Décollement coefficient of friction	0.1 – 1, in 0.1 increments	*Byerlee* [1978]
F	Décollement strength		
β	Dip angle of décollement	Calculated	
		Environmental	
g	Acceleration due to gravity	3.7 m s^{-2}	*Esposito et al.* [1992]
ρ_f	Density of the Martian atmosphere	0.0176 kg m^{-3}	*Schofield et al.* [1997]

pore fluid pressure, g is the acceleration due to gravity, and z is the depth) [*Hubbert and Rubey*, 1959], S_b is the décollement cohesion, H is the maximum vertical thickness of the wedge determined from topographic profiles, Φ is the angle of internal friction for the wedge (where $\Phi = \tan^{-1} \mu$), and C is cohesion of the wedge. Once a crustal section has been compressed sufficiently for its geometry to achieve a critical taper, given by the quantity $(\alpha + \beta)$, it slides along the basal décollement, whereas no significant translation occurs for tapers smaller than or larger than the critical taper.

[18] A variety of terrestrial settings and locations has been investigated using CTWM. Subaerial wedges, such as those in the Himalaya and Taiwan, as well as submarine wedges, such as the Java Trench, the Makran wedge, and the Aleutians, have been characterized and analyzed using CTWM. Measured surface topographic slopes (α) and décollement dip angles (β) (Figure 5) for several terrestrial critical taper wedges are: Himalaya $\alpha = 4.0°$, $\beta = 3.0°$ [*Ohta and Akiba*, 1973; *Seeber et al.*, 1981], Taiwan $\alpha = 2.9°$, $\beta = 6.0°$ [*Suppe*, 1980, 1981; *Davis et al.*, 1983], Java Trench south of Bali $\alpha = 3.1°$, $\beta = 6.6°$ [*Hamilton*, 1979], Makran wedge in the Gulf of Oman $\alpha = 1.6°$, $\beta = 2.0°$ [*White and Ross*, 1979], Peru Trench $\alpha = 3.8°$, $\beta = 5.9°$ [*Keller et al.*, 1979], Guatemala $\alpha = 5.7°$, $\beta = 2.5°$ [*Seely et al.*, 1974, pp. 249–260], Oregon $\alpha = 2.1°$, $\beta = 6.0°$ [*Snavely et al.*, 1980], and eastern Aleutians in the Gulf of Alaska $\alpha = 3.0°$, $\beta = 4.5°$ [*von Huene et al.*, 1979].

[19] *Davis et al.* [1983] calculated the pore fluid pressure ratios for several terrestrial wedges, both subaerial and submarine. Hydrostatic pressure in an aquifer corresponds to a pore fluid pressure ratio $\lambda \approx 0.33$, whereas lithostatic pressure corresponds to $\lambda = 1$ [*Hubbert and Rubey*, 1959]. Using values obtained by *Davis et al.* [1983] for Taiwan ($\mu_b = 0.85$, $\mu = 1.03$) and the geometry of the wedges as determined by other workers and listed above include: Himalaya $\lambda = 0.76$, Java Trench south of Bali $\lambda = 0.7$, Makran wedge in the Gulf of Oman $\lambda = 0.98$, Peru Trench $\lambda = 0.6$, Guatemala $\lambda = 0.7$, Oregon $\lambda = 0.9$, and eastern Aleutians in the Gulf of Alaska $\lambda = 0.88$. Their calculated pore fluid pressures are in agreement with the observed values for wedges where observations are available: Makran $\lambda = \sim 1$ (as noted by *Davis et al.* [1983]), Guatemala $\lambda =$ "high" [*Aubouin et al.*, 1982], Oregon $\lambda = 0.85$ [*Moore and von Huene*, 1980], and Aleutians $\lambda = \sim 0.87$ [*Hottman et al.*, 1979]. Generally, the predicted pore fluid pressure ratios are well in excess of hydrostatic ($\lambda \gtrsim 0.33$) and terrestrial critical taper wedges require $\mu = 1.03$, $\mu_b = 0.85$, and $\lambda = 0.68$–0.98 [*Davis et al.*, 1983]. Brittle rock strengths measured in the laboratory (e.g., maximum static friction coefficient $\mu = 0.7$ for gabbro, $\mu = 0.8$ for marble, and $\mu = 0.7$ for granite, sandstone, and quartzite [*Paterson and Wong*, 2005, pp. 166–172]) are consistent with those observed in the Taiwan fold-and-thrust belt ($\mu = 0.85$–1.03) [*Davis et al.*, 1983].

[20] *Suppe and Connors* [1992] were the first to apply CTWM to another planet. They identified a number of possible fold-and-thrust belts on Venus, including Artemis Chasma, Maxwell Montes, and Uorsar Rupes [*Suppe and Connors*, 1992]. Here, typical fold-belt widths were found to be on the order of 100 km, with Maxwell Montes being the widest belt, with a width of 500 km [*Suppe and Connors*, 1992]. Many of the fold belts are located at the margins of plateaus, with others occurring at the margins of larger deformed coronae [*Suppe and Connors*, 1992]. On Venus, critical taper wedges appear to have similar cross-sectional geometries to those on Earth, with the addition of a flat plateau region, located behind the less deformed shallowly sloping toe and narrow region of steep slope (5°–20°), where the inferred base of the wedge and décollement are both deforming by ductile flow as a result of the high surface temperatures and lack of water [*Suppe and Connors*, 1992; *Williams et al.*, 1994]. The absence of water vapor in the Venusian atmosphere [*Kaula*, 1990] implies that the rheological properties for dry basaltic or diabasic crust ($\lambda = 0$) are appropriate for Venusian CTWM calculations. The coefficient of friction of the décollement (μ_b) was assumed to be equal to that of the wedge (μ) at 0.6 [*Williams et al.*, 1994] for these calculations. Maximum surface slopes for

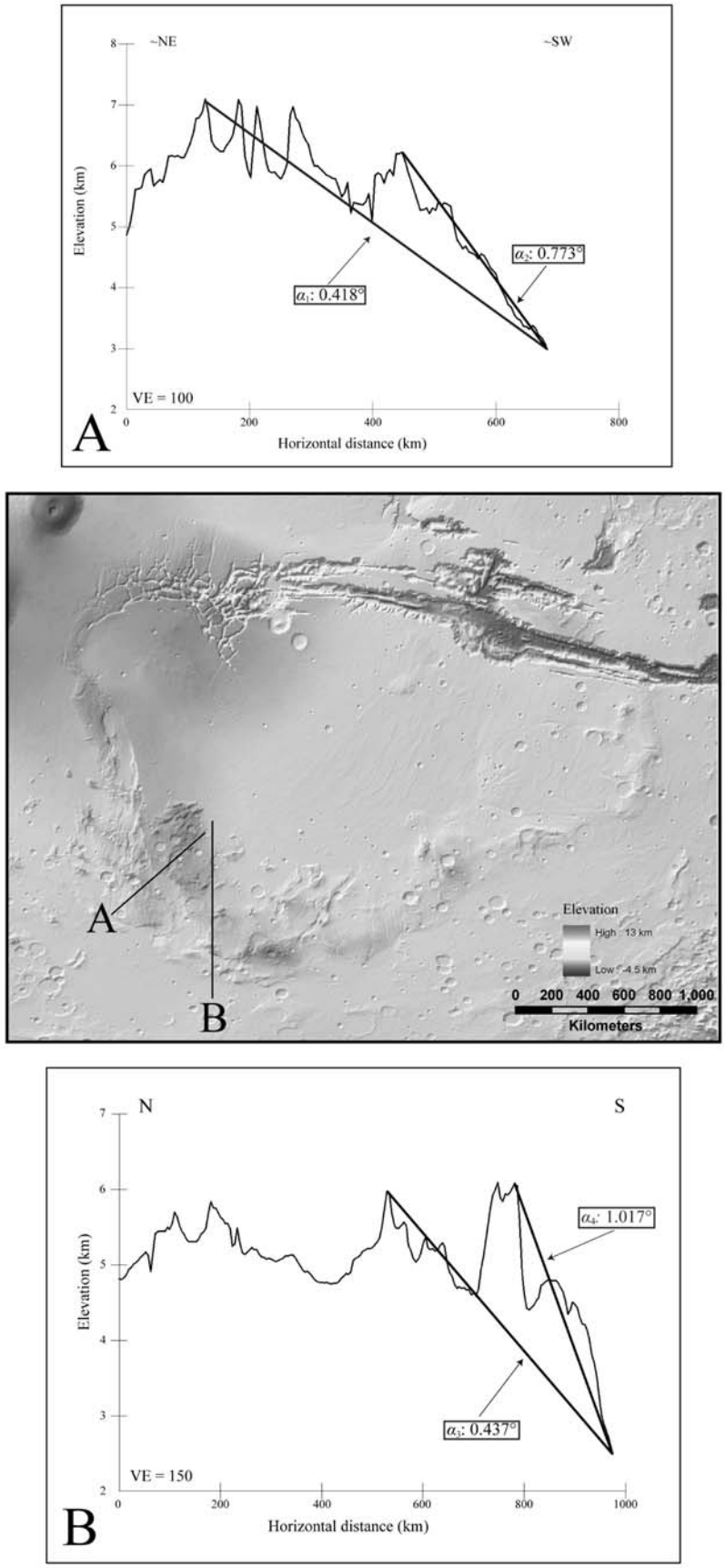
~NE
~SW
Elevation (km)
α_2: 0.773°
α_1: 0.418°
VE = 100
A
Horizontal distance (km)
A
B
Elevation
High 13 km
Low -4.5 km
0 200 400 600 800 1,000
Kilometers
N
S
Elevation (km)
α_4: 1.017°
α_3: 0.437°
VE = 150
B
Horizontal distance (km)

Figure 6

brittle wedges on Venus were found to be 10°–20° for possible décollement dips of 5°–10° [*Suppe and Connors*, 1992]. The results of *Williams et al.* [1994] show that the addition of ductile behavior to the frictional CTWM theory reproduces the surface topography of Maxwell Montes and Uorsar Rupes reasonably well, as it does with the topography of the Andes orogenic belt on the Earth. While it has been inferred that these areas on Venus have deformed as critical taper wedges, no direct measurements exist to confirm the presence of a basal décollement. In addition, the requirement of large-scale lithospheric mobility resulting in ~100–200 km of horizontal shortening may be difficult to demonstrate on Venus.

[21] Fold-and-thrust belts on Earth and Venus exhibit common properties and geometries including (1) a basal detachment surface or décollement that dips toward the interior of the belt along which the wedge slides, (2) large horizontal shortening in the material above the décollement, and (3) the deformed material forms a wedge geometry (Figure 5) [*Chapple*, 1978; *Davis et al.*, 1983; *Suppe and Connors*, 1992]. An increase in décollement friction (μ_b) increases the angle of the critical taper ($\alpha + \beta$), while an increase in the internal friction in the wedge (μ) decreases the critical taper; as the pore fluid pressure ratio (λ) increases, the surface slope (α) decreases toward horizontal ($\alpha = 0°$), reducing the critical taper [*Davis et al.*, 1983].

[22] Formation of the Thaumasia Highlands as an orogenic belt implicitly assumes CTWM and the requirement of a fully developed and slipping décollement at depth, requiring that the topographic slope across the Thaumasia Highlands defines a critical taper. In order to test the orogenic belt hypothesis for the Thaumasia Highlands, several topographic profiles derived from Mars Orbiter Laser Altimeter (MOLA) digital elevation models (DEMs) were measured across the Thaumasia Highlands (Figure 6). Transects were measured in locations that avoided volcanoes or large craters. Two surface slopes (α) were measured from each of two transects and used in the calculations (Figure 6). Four slopes were obtained from these transects: $\alpha = 0.418°$, 0.773° (Figure 6a) and $\alpha = 0.437°$, 1.017° (Figure 6b). Slopes were taken from the highest points of elevation not associated with objects such as crater rims to the lowest elevation point of the profile.

[23] To determine under what conditions critical taper wedges could form in the Thaumasia Highlands, key physical properties, such as μ_b, μ, and λ, were varied within the ranges for these variables (Table 1) suggested by terrestrial and Venusian values (i.e., Earth: $\mu_b = 0.85$, $\mu = 1.03$, and $\lambda = 0.68$–0.98; Venus: $\mu_b = \mu = 0.6$, and $\lambda = 0$). The dip angle of a hypothetical décollement (β) was calculated using the measured surface slopes and the values for μ_b, μ, and λ listed in Table 1 in equations (1)–(3). Values for décollement dip angle of $0° < \beta < 10°$ were considered to be most reasonable, since observed values of β on Earth have been found to be ≤10° [*Davis et al.*, 1983]. Of the 2424 cases obtained from varying μ_b, μ, and λ for each measured α, 777 cases were found where $0° < \beta < 10°$.

5. Results and Discussion

[24] Results of the critical taper wedge calculations are illustrated in Figures 7 and 8. For Figures 7 and 8, the graphs show the calculated décollement dip angle versus the wedge friction coefficient with the friction coefficient of the décollement varied between 0.1 and 0.9 (shown in upper right hand corner of each box). Figure 7 shows results for the smallest surface slope measured ($\alpha_1 = 0.418°$) and Figure 8 shows results for the largest surface slope measured in this study ($\alpha_4 = 1.017°$) across the Thaumasia Highlands. Décollement dip angles for reasonable values of décollement friction (0.6 – 0.85) [*Byerlee*, 1978] are shown by arrows at the left of each box. For $\mu_b = 0.1 – 0.4$, these dip angles range between ~0° and 10° (Figures 7 and 8), which are similar to terrestrial décollement friction coefficients [*Davis et al.*, 1983]. For $\mu_b = 0.6 – 0.9$, however, the calculated décollement dip angles range between 8° and 25° (Figures 7 and 8), which are larger than most terrestrial décollement dip values ($0° < \beta < 10°$) [*Davis et al.*, 1983].

[25] The results suggest that subhorizontal décollements, having dip values $\ll 5°$, would be unlikely under the Thaumasia Highlands, even under high pore fluid pressure ratio conditions (Figures 7 and 8). Additionally, for reasonable values of wedge and décollement friction ($\mu \geq 0.6$ [*Byerlee*, 1978]; Figures 7 and 8, bottom) the predicted décollement dips beneath the Thaumasia Highlands would be between 8° and 25°, steeper than the low-angle dips of terrestrial fold-and-thrust belts.

[26] The geometry of potential orogenic wedges in the Thaumasia Highlands requires unusually low values of décollement friction ($\mu_b < 0.4$) if the Thaumasia Highlands were to have formed as an orogenic wedge. Critical taper wedges on Earth are characterized by strong décollements ($\mu_b = 0.85$), consistent with Byerlee friction of common rock types such as basalt with frictional sliding along the base [*Davis et al.*, 1983]. Weaker décollements on Earth, and potentially on Mars, could arise in association with serpentinite fault gouge (with values as low as $\mu = 0.15$) or dry montmorillonite gouge (with values as low as $\mu = 0.08$) [*Paterson and Wong*, 2005, pp. 166–172]. The coefficient of friction for clay-rich gouges along the San Andreas and Hayward fault zones, for example, has been found to be between 0.21 and 0.55 [*Paterson and Wong*, 2005]; values on the low end of this spectrum are in the range required by our calculations ($0.1 < \mu_b < 0.4$), but the larger values are stronger than those necessary for basal sliding of critical taper wedges on Mars. Creation of large regional-scale décollements on Mars containing sufficiently large concentrations of either serpentinite or montmorillonite appears therefore to require special conditions. Although several clay minerals have recently been discovered on Mars (e.g.,

Figure 6. Topographic profiles extracted from a MOLA DEM and their locations in the Thaumasia Highlands. Profile locations in Thaumasia Highlands shown as solid black lines in lower left (southwest) portion of image (middle). Measured average slope is shown near each profile segment. (a) Vertical exaggeration: 100:1. H values for $\alpha_1 = 4171$ m, $\alpha_2 = 3250$ m; (b) Vertical exaggeration: 150:1. H values for $\alpha_3 = 3353$ m, $\alpha_4 = 3470$ m.

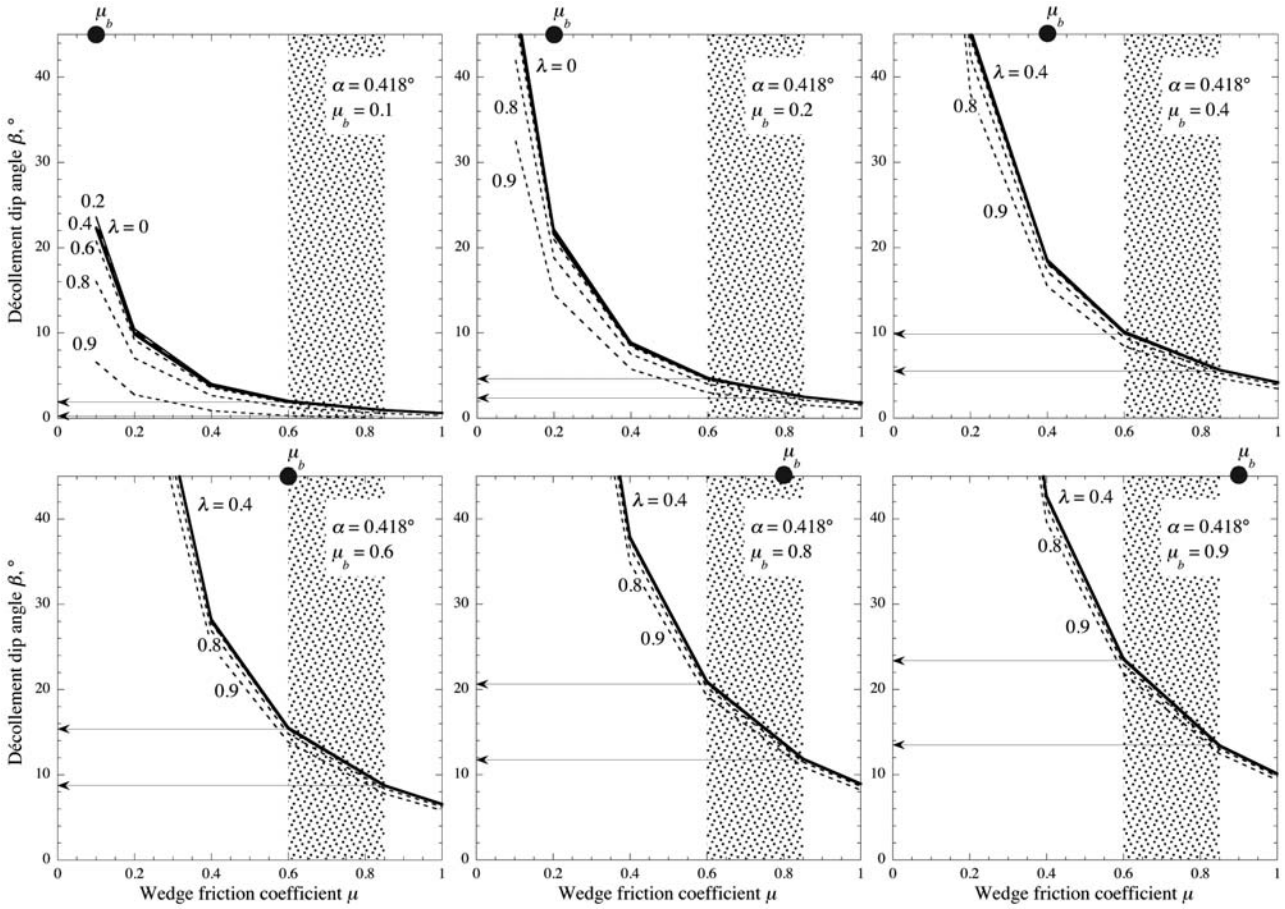

Figure 7. Plot showing the change in calculated décollement dip angle, β, when wedge friction coefficient (μ), pore fluid pressure ratio (λ), and décollement coefficient of friction (μ_b) are varied. All calculations are for surface slope $\alpha_1 = 0.418°$ (Figure 6). Thin solid curves are for dry conditions ($\lambda = 0$), bold solid curves are for hydrostatic conditions ($\lambda = 0.4$), and short dashed curves are for overpressured conditions ($\lambda > 0.4$). Shaded areas show reasonable values for wedge friction ($\mu = 0.6 – 0.85$) [*Byerlee*, 1978]. Arrows show predicted values of décollement dip angle (β) given the likely range of μ.

nontronite, saponite, montmorillonite, and kaolinite) [*Bibring et al.*, 2006; *Mustard et al.*, 2008], they are not associated with faults and are presently known to be confined to light-toned near-surface deposits and areas of small spatial extent, such as the flanks of the outflow channel of Mawrth Valles, crater ejecta deposits [*Mustard et al.*, 2008], and in Nili Fossae [*Bibring et al.*, 2006].

[27] The presence of a large quantity of salt has been hypothesized to underlie part or all of the Thaumasia Plateau by *Montgomery et al.* [2009]. The coefficient of dynamic friction for halite is in the range of $\mu_k = 0.53–1.08$ [*Mair et al.*, 2006], with ~0.6 being the approximate value for a mixture of salt and silicates (e.g., evaporite-rich sediments). Décollement dip angles for this value of friction are between 8 and 25° (Figures 7 and 8), again larger than those observed in most terrestrial fold-and-thrust belts. Although halite has not been identified in spectra available for Mars, the strength of the décollement would vary first, with the presence of evaporites and second, their concentration rather than the type of evaporite(s) present. In the event that such a salt body were present beneath the Thaumasia Plateau, the attributes of salt décollement fold-and-thrust belts, such as inconsistent vergence direction and the presence of salt-cored anticlines, should be recognizable and could be used to identify the presence of salt at depth in these terranes [*Davis and Engelder*, 1985; *Costa and Vendeville*, 2002]. Detailed studies of the Thaumasia Highlands indicate instead a consistent vergence of thrust faults [*Plescia et al.*, 1980; *Plescia and Saunders*, 1982; *Watters*, 1993, *Dohm and Tanaka*, 1999; *Grott et al.*, 2007] and there is no evidence for salt-cored anticlines in imaging, spectral, or gravity data, implying that any evaporites in the Martian subsurface were not important in CTWM-related deformation.

[28] High pore fluid pressure ratios may have been achieved on Mars by pressurization of aquifers resulting from several mechanisms. Overpressurization ($\lambda > 0.33$) may result from compaction of aquifers contained within low-permeability sediments due to compressional tectonics or the weight of the overburden [*Hubbert and Rubey*, 1959], as has been suggested to have occurred below Olympus Mons [*McGovern and Morgan*, 2009]. In a second possibility, the brittle plastic transition in Tharsis could migrate toward the surface as deep portions of the crust reached thermal equilibrium [*Andrews-Hanna et al.*, 2007]. As buried aquifers underwent the transition to the plastic regime, the water contained within them would have been

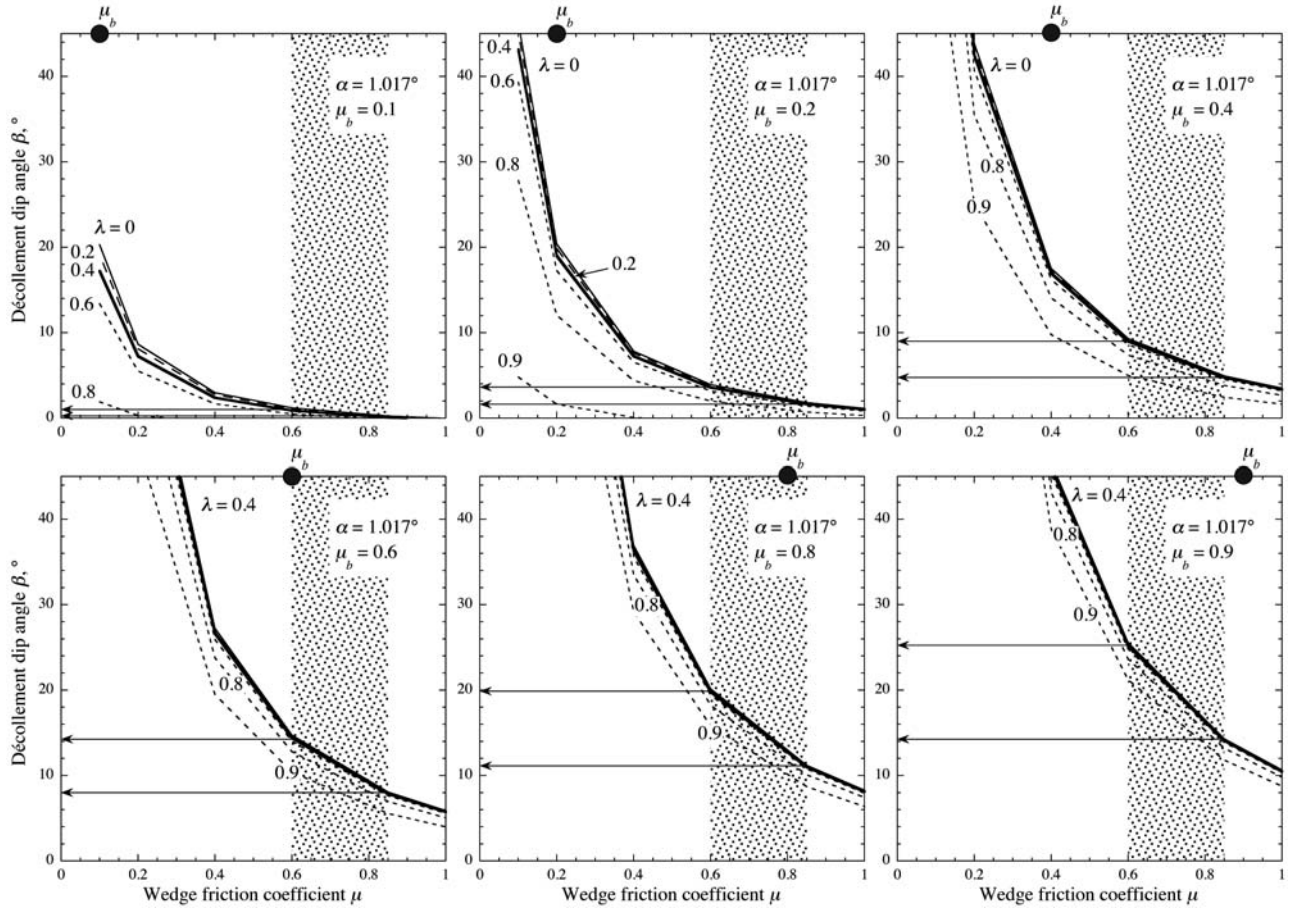

Figure 8. Plot showing the change in calculated décollement dip angle, β, when wedge friction coefficient (μ), pore fluid pressure ratio (λ), and décollement coefficient of friction (μ_b) are varied. All calculations are for surface slope $\alpha_4 = 1.017°$ (Figure 6). Thin solid curves are for dry conditions ($\lambda = 0$), bold solid curves are for hydrostatic conditions ($\lambda = 0.4$), and short dashed curves are for overpressured conditions ($\lambda > 0.4$). Shaded areas show reasonable values for wedge friction ($\mu = 0.6 – 0.85$) [*Byerlee*, 1978]. Arrows show predicted values of décollement dip angle (β) given the likely range of μ.

subjected to the full lithostatic pressure [*Andrews-Hanna et al.*, 2007], resulting in aquifers pressurized in excess of hydrostatic. Rapid climate change (from warm and wet to present-day cold and dry conditions) and resultant freezing and cryosphere thickening may also have briefly resulted in pore fluid pressure ratios exceeding lithostatic, but as the rate of cryosphere thickening decreases, the pressure in the aquifers would gradually reduce and the pore pressure would ultimately return to sublithostatic pore fluid pressure ratios [*Hanna and Phillips*, 2005]. Tectonic pressurization of saturated aquifers near Athabasca Valles and Mangala Valles from single tectonic events apparently resulted in pore fluid pressure ratios that exceeded lithostatic pressures [*Hanna and Phillips*, 2006]. These results suggest that, although locally high pore fluid pressure ratios may have developed on Mars, they are likely not sufficient in themselves to promote orogenic belts having a critical taper.

[29] Perhaps a more intractable shortcoming of the orogenic belt hypothesis for the formation of the Thaumasia Highlands is the requirement for significant horizontal shortening of the lithosphere before deformation by critical taper wedge mechanics begins. In particular, horizontal shortening in excess of several hundred km is required for lithosphere to deform into critical taper geometries. On Earth, plate convergence at subduction zones provides both the needed horizontal motions as well as the "backstop" required for stratigraphic sequences to deform into critical tapers [e.g., *Davis et al.*, 1983; *Dahlen*, 1990; *Nemčok et al.*, 2005, pp. 26–45]. On Mars, no evidence has been recognized to support the notion that lithosphere upslope of potential Martian critical taper wedges (or orogenic belts) has been shortened by hundreds of km. In the Thaumasia region, such southward translation of lithosphere would require extremely large-scale strike-slip offsets and large-scale lithospheric extension in the Claritas Fossae-Noctis Labyrinthus-Valles Marineris region. Although extension and rifting do occur in these areas, southward translation of lithosphere toward the Thaumasia Highlands having the large magnitudes required to achieve critical taper wedge geometries would greatly exceed the magnitudes of extensional strains in those areas [e.g., *Golombek and Phillips*, 2010]. Further, no mechanism exists to produce southward lithospheric translation in Thaumasia, given average regional slopes of 0.1° or less [cf. *Montgomery et al.*, 2009]. Inter-

estingly, *Morgan and McGovern* [2005] and *McGovern and Morgan* [2009] find that the flanks of Olympus Mons and other large planetary volcanoes may behave analogously to critical taper wedges. In this case, however, large horizontal tectonic compression does not provide the deformation mechanism. Rather, the weight of the volcano itself appears sufficient to produce the observed deformation. Consequently, thrust faulting as a result of critical taper wedge mechanics is unlikely in Thaumasia given the rather stringent requirements for weak basal décollements, high pore fluid pressure ratios, and large horizontal shortening in excess of observations.

[30] The results show that, in general, regional slopes in the Thaumasia region are too small for the topography to achieve a critical wedge taper for reasonable values of décollement dip angle, pore fluid pressure ratios, and rock properties. These results imply that lobate scarps elsewhere on Mars [e.g., *Watters*, 1993] probably also accommodate lithospheric shortening as discrete structures in response to a regional stress state rather than as an integrated set within critical taper orogenic wedges.

[31] These findings also have implications for the rheologic properties of Martian lithosphere under Thaumasia during the Noachian. *Grott and Breuer* [2008] infer that a layer of weaker crust separates the mechanically stronger crustal and mantle layers early in Mars' history, but cooling of the planet causes this layer to diminish at later times. A weak wet mantle rheology is appropriate to match constraints on Mars' thermal and crustal evolution, such as the majority of the crust being in place by 4 Ga [*Hauck and Phillips*, 2002] and an average crustal thickness of 50 km [*Zuber et al.*, 2000]. The lack of a décollement under the Thaumasia Highlands independently supports results from *Okubo and Schultz* [2003], which show that the base of the Tharsis load was effectively welded to the subjacent Noachian crust during the Noachian to early Hesperian. Tharsis tectonics likely reflects lithosphere-scale thick-skinned deformation, as opposed to thin-skinned deformation above a slipping décollement [*Okubo and Schultz*, 2003].

6. Conclusions

[32] The hypothesis of orogenesis involving critical taper wedge mechanics in the Thaumasia Highlands region of Mars is tested in this paper. Using MOLA topography and representative values of rock frictional strength, the Thaumasia Highlands and associated marginal thrust faults are not consistent with a critical taper orogenic wedge as has been proposed in the literature. For slope angles of 0.418–1.017° measured across the Thaumasia Highlands and values of friction coefficient typical of basaltic rock sequences, a critical taper wedge would require sustained values of pore fluid pressure ratio substantially in excess of hydrostatic ($0.33 < \lambda < 0.9$) along with unusually low values of friction coefficient along a putative basal décollement ($\mu_b = 0.1 – 0.4$; Figures 7 and 8). Although deformation in this area during Noachian time may have been associated with some nonzero level of pore fluid pressure, and although some occurrences of clay minerals have been recently reported from various areas of Mars, the specific combination of conditions that would need to exist during the time of the Thaumasia Highlands deformation appears unlikely. In addition, a mechanism to provide both the "backstop" and the large values of lithospheric horizontal shortening (on the order of several hundred km, based on values from Earth) required to promote slopes consistent with critical taper wedges has not been demonstrated in the literature. Correspondingly, values of extensional deformation to the north, as inferred by detailed investigations of graben sets that would need to balance the implied critical taper deformation in the Thaumasia Highlands are too low by orders of magnitude, implying minimal southward translation of the Thaumasia Plateau. Thrust faulting along the southern margin of the Thaumasia Highlands appears instead to be associated with localized deformation; formation mechanisms that do not require large horizontal translation of Martian lithosphere, such as flexure, may be more consistent with the topography and tectonics of the Thaumasia Highlands.

[33] **Acknowledgments.** This paper benefited from thoughtful reviews by Jeff Andrews-Hanna and Álvaro Márquez. The authors thank David Prudic for helpful discussion about λ and Robert Lillis for discussion about the Martian crustal magnetic field. This work was supported by a grant from NASA's Mars Data Analysis Program to R.A.S.

References

Allemand, P., and P. G. Thomas (1995), Localization of Martian ridges by impact craters: Mechanical and chronological implications, *J. Geophys. Res.*, *100*, 3251–3262, doi:10.1029/94JE03081.

Alonso, J. L., and J. A. Pulgar (2004), Estructura alpina de la Cordillera Cantábrica: Generalidades, in *Geología de España*, edited by J. A. Vera, pp. 332–334, IGM-SGE, Madrid, Spain.

Alonso, J. L., J. A. Pulgar, J. C. García-Ramos, and P. Barba (1996), Tertiary basins and Alpine tectonics in the Cantabrian Mountains (NW Spain), in *Tertiary Basins of Spain: The Stratigraphic Record of Crustal Kinematics*, edited by P. F. Friend and C. J. Dabrio, pp. 214–227, Cambridge Univ. Press, Cambridge, U. K.

Anderson, R. C., J. M. Dohm, M. P. Golombek, A. F. C. Haldemann, B. J. Franklin, K. L. Tanaka, J. Lias, and B. Peer (2001), Primary centers and secondary concentrations of tectonic activity through time in the western hemisphere of Mars, *J. Geophys. Res.*, *106*, 20,563–20,585.

Andrews-Hanna, J. C. (2009), A mega-landslide on Mars, *Nat. Geosci.*, *2*, 248–249, doi:10.1038/ngeo483.

Andrews-Hanna, J. C., R. J. Phillips, and M. T. Zuber (2007), Meridiani Planum and the global hydrology of Mars, *Nature*, *446*, 163–166, doi:10.1038/nature05594.

Andrews-Hanna, J. C., M. T. Zuber, and S. A. Hauck II (2008), Strike-slip faults on Mars: Observations and implications for global tectonics and geodynamics, *J. Geophys. Res.*, *113*, E08002, doi:10.1029/2007JE002980.

Anguita, F., A.-F. Farelo, V. López, C. Mas, M.-J. Muñoz-Espadas, A. Márquez, and J. Ruiz (2001), Tharsis dome, Mars: New evidence for Noachian-Hesperian thick-skin and Amazonian thin-skin tectonics, *J. Geophys. Res.*, *106*, 7577–7589, doi:10.1029/2000JE001246.

Anguita, F., C. Fernández, G. Cordero, S. Carrasquilla, J. Anguita, A. Núñez, S. Rodríguez, and J. García (2006), Evidences for a Noachian-Hesperian orogeny in Mars, *Icarus*, *185*, 331–357, doi:10.1016/j.icarus.2006.07.026.

Ansan, V., and N. Mangold (2006), New observations of Warrego Valles, Mars: Evidence for precipitation and surface runoff, *Planet. Space Sci.*, *54*, 219–242, doi:10.1016/j.pss.2005.12.009.

Arkani-Hamed, J. (2004), Timing of the Martian core dynamo, *J. Geophys. Res.*, *109*, E03006, doi:10.1029/2003JE002195.

Aubouin, J., et al. (1982), Leg 84 of the Deep Sea Drilling Project, subduction without accretion: Middle America Trench off Guatemala, *Nature*, *297*, 458–460, doi:10.1038/297458a0.

Banerdt, W. B., M. P. Golombek, and K. L. Tanaka (1992), Stress and tectonics on Mars, in *Mars*, edited by H. H. Keiffer et al., pp. 249–297, Univ. of Ariz. Press, Tucson.

Bibring, J-P., et al. (2006), Global mineralogical and aqueous Mars history derived from OMEGA/Mars Express data, *Science*, *312*, 400–404, doi:10.1126/science.1122659.

Borgia, A., J. Burr, W. Montero, L. D. Morales, and G. A. Alvarado (1990), Fault propagation folds induced by gravitational failure and slumping of the central Costa Rica volcanic range: Implications for large

terrestrial and Martian volcanic edifices, *J. Geophys. Res.*, *95*, 14,357–14,382, doi:10.1029/JB095iB09p14357.

Borraccini, F., G. D. Achille, G. G. Ori, and F. C. Wezel (2007), Tectonic evolution of the eastern margin of the Thaumasia Plateau (Mars) as inferred from detailed structural mapping and analysis, *J. Geophys. Res.*, *112*, E05005, doi:10.1029/2006JE002866.

Byerlee, J. (1978), Friction of rocks, *Pure Appl. Geophys.*, *116*, 615–626, doi:10.1007/BF00876528.

Chapple, W. M. (1978), Mechanics of thin-skinned fold-and-thrust belts, *Geol. Soc. Am. Bull.*, *89*, 1189–1198, doi:10.1130/0016-7606(1978)89<1189:MOTFB>2.0.CO;2.

Chicarro, A. F., P. H. Schultz, and P. Masson (1985), Global and regional ridge patterns on Mars, *Icarus*, *63*, 153–174, doi:10.1016/0019-1035(85)90025-9.

Connerney, J. E. P., M. H. Acuña, N. F. Ness, G. Kletetschka, D. L. Mitchell, R. P. Lin, and H. Reme (2005), Tectonic implications of Mars crustal magnetism, *Proc. Natl. Acad. Sci. U. S. A.*, *102*, 14,970–14,975, doi:10.1073/pnas.0507469102.

Costa, E., and B. C. Vendeville (2002), Experimental insights on the geometry and kinematics of fold-and-thrust belts above a weak, viscous evaporitic décollement, *J. Struct. Geol.*, *24*, 1729–1739, doi:10.1016/S0191-8141(01)00169-9.

Courtillot, V. E., C. J. Allegre, and M. Mattauer (1975), On the existence of lateral relative motions on Mars, *Earth Planet. Sci. Lett.*, *25*, 279–285, doi:10.1016/0012-821X(75)90242-3.

Dahlen, F. A. (1990), Critical taper model of fold-and-thrust belts and accretionary wedges, *Annu. Rev. Earth Planet. Sci.*, *18*, 55–99, doi:10.1146/annurev.ea.18.050190.000415.

Dahlen, F. A., J. Suppe, and D. Davis (1984), Mechanics of fold-and-thrust belts and accretionary wedges: Cohesive Coulomb theory, *J. Geophys. Res.*, *89*, 10,087–10,101, doi:10.1029/JB089iB12p10087.

Davis, D. M., and T. Engelder (1985), The role of salt in fold-and-thrust belts, in *Collision Tectonics: Deformation of Continental Lithosphere*, edited by N. L. Carter and S. Uycda, *Tectonophysics*, 119, 67–88.

Davis, D., J. Suppe, and F. A. Dahlen (1983), Mechanics of fold-and-thrust belts and accretionary wedges, *J. Geophys. Res.*, *88*, 1153–1172, doi:10.1029/JB088iB02p01153.

Dohm, J. M., and K. L. Tanaka (1999), Geology of the Thaumasia region, Mars: Plateau development, valley origins, and magmatic evolution, *Planet. Space Sci.*, *47*, 411–431, doi:10.1016/S0032-0633(98)00141-X.

Dohm, J. M., K. L. Tanaka, and T. M. Hare (2001), Geologic, paleotectonic, and paleoerosional maps of the Thaumasia region, Mars (1:5,000,000), *U.S. Geol. Surv. Misc. Inv. Ser. Map I–2650*.

Esposito, P. B., W. B. Banerdt, G. F. Lindal, W. L. Sjogren, M. A. Slade, B. G. Bills, D. E. Smith, and G. Balmino (1992), Gravity and topography, in *Mars*, edited by H. H. Keiffer et al., pp. 209–248, Univ. of Ariz. Press, Tucson.

Frey, H. V. (1979), Thaumasia: A fossilized early forming Tharsis uplift, *J. Geophys. Res.*, *84*, 1009–1023, doi:10.1029/JB084iB03p01009.

Golombek, M. P., and R. J. Phillips (2010), Mars tectonics, in *Planetary Tectonics*, edited by T. R. Watters and R. A. Schultz, pp. 183–232, Cambridge Univ. Press, Cambridge, U. K.

Grott, M., and D. Breuer (2008), The evolution of the Martian elastic lithosphere and implications for crustal and mantle rheology, *Icarus*, *193*, 503–515, doi:10.1016/j.icarus.2007.08.015.

Grott, M., E. Hauber, S. C. Werner, P. Kronberg, and G. Neukum (2007), Mechanical modeling of thrust faults in the Thaumasia region, Mars, and implications for the Noachian heat flux, *Icarus*, *186*, 517–526, doi:10.1016/j.icarus.2006.10.001.

Hamilton, W. (1979), Tectonics of the Indonesian region, *U.S. Geol. Surv. Prof. Pap.*, *1078*, 345 pp.

Hanna, J. C., and R. J. Phillips (2005), Hydrological modeling of the Martian crust with application to the pressurization of aquifers, *J. Geophys. Res.*, *110*, E01004, doi:10.1029/2004JE002330.

Hanna, J. C., and R. J. Phillips (2006), Tectonic pressurization of aquifers in the formation of Mangala and Athabasca Valles, Mars, *J. Geophys. Res.*, *111*, E03003, doi:10.1029/2005JE002546.

Hartmann, W. K., and G. Neukum (2001), Cratering chronology and the evolution of Mars, *Space Sci. Rev.*, *96*, 165–194, doi:10.1023/A:1011945222010.

Hauber, E., and P. Kronberg (2005), The large Thaumasia graben on Mars: Is it a rift? *J. Geophys. Res.*, *110*, E07003, doi:10.1029/2005JE002407.

Hauck, S. A., II, and R. J. Phillips (2002), Thermal and crustal evolution of Mars, *J. Geophys. Res.*, *107*(E7), 5052, doi:10.1029/2001JE001801.

Head, J. W., M. A. Kreslavsky, and S. Pratt (2002), Northern lowlands of Mars: Evidence for widespread volcanic flooding and tectonic deformation in the Hesperian period, *J. Geophys. Res.*, *107*(E1), 5003, doi:10.1029/2000JE001445.

Hottman, C. E., J. H. Smith, and W. R. Purcell (1979), Relationship among Earth stresses, pore pressure, and drilling problems offshore Gulf of Alaska, *JPT J. Pet. Technol.*, *31*, 1477–1484, doi:10.2118/7501-PA.

Hubbert, M. K., and W. W. Rubey (1959), Role of fluid pressure in mechanics of overthrust faulting: 1. Mechanics of fluid-filled porous solids and its application to overthrust faulting, *Geol. Soc. Am. Bull.*, *70*, 115–166, doi:10.1130/0016-7606(1959)70[115:ROFPIM]2.0.CO;2.

Johnson, C. L., and R. J. Phillips (2005), Evolution of the Tharsis region of Mars: Insights from magnetic field observations, *Earth Planet. Sci. Lett.*, *230*, 241–254, doi:10.1016/j.epsl.2004.10.038.

Kaula, W. M. (1990), Venus: A contrast in evolution to Earth, *Science*, *247*, 1191–1196, doi:10.1126/science.247.4947.1191.

Keller, B., B. T. R. Lewis, C. Meeder, C. Helsley, and R. P. Meyer (1979), Explosion seismology studies of active and passive continental margins, in *Geological and Geophysical Investigation of Continental Margins*, edited by J. S. Watkins et al., *AAPG Mem.*, *29*, 443–451.

Knapmeyer, M., J. Oberst, E. Hauber, M. Wählisch, C. Deuchler, and R. Wagner (2006), Working models for spatial distribution and level of Mars' seismicity, *J. Geophys. Res.*, *111*, E11006, doi:10.1029/2006JE002708.

Knapmeyer, M., S. Schneider, M. Misun, M. Wählisch, and E. Hauber (2008), An extended global inventory of Mars surface faults, *Geophys. Res. Abstr.*, *10*, EGU2008-A-03574.

Lillis, R. J., H. V. Frey, and M. Manga (2008a), Rapid decrease in Martian crustal magnetization in the Noachian era: Implications for the dynamo and climate of early Mars, *Geophys. Res. Lett.*, *35*, L14203, doi:10.1029/2008GL034338.

Lillis, R. J., H. V. Frey, M. Manga, D. L. Mitchell, R. P. Lin, M. H. Acuña, and S. W. Bougher (2008b), An improved crustal magnetic field map of Mars from electron reflectometry: Highland volcano magmatic history and the end of the Martian dynamo, *Icarus*, *194*, 575–596, doi:10.1016/j.icarus.2007.09.032.

Lillis, R. J., J. Dufek, J. E. Bleacher, and M. Manga (2009), Demagnetization of crust by magmatic intrusion near the Arsia Mons volcano: Magnetic and thermal implications for the development of the Tharsis province, Mars, *J. Volcanol. Geotherm. Res.*, *185*, 123–138, doi:10.1016/j.jvolgeores.2008.12.007.

Lin, J., and R. S. Stein (2004), Stress triggering in thrust and subduction earthquakes, and stress interaction between the southern San Andreas and nearby thrust and strike-slip faults, *J. Geophys. Res.*, *109*, B02303, doi:10.1029/2003JB002607.

Lucchitta, B. K., A. S. McEwen, G. D. Clow, P. E. Geissler, R. B. Singer, R. A. Schultz, and S. W. Squyres (1992), The canyon system on Mars, in *Mars*, edited by H. H. Keiffer et al., pp. 453–492, Univ. of Ariz. Press, Tucson.

Mair, K., F. Renard, and O. Gunderson (2006), Thermal imaging on simulated faults during frictional sliding, *Geophys. Res. Lett.*, *33*, L19301, doi:10.1029/2006GL027143.

Mangold, N., and V. Ansan (2006), Detailed study of an hydrological system of valleys, a delta and lakes in the Southwest Thaumasia region, Mars, *Icarus*, *180*, 75–87, doi:10.1016/j.icarus.2005.08.017.

Mangold, N., P. Allemand, P. G. Thomas, and G. Vidal (2000), Chronology of compressional deformation on Mars: Evidence for a single and global origin, *Planet. Space Sci.*, *46*, 345–356.

McGill, G. E. (1979), Geologic map of Thaumasia quadrangle, Mars (1:5,000,000), *U.S. Geol. Surv. Misc. Inv. Map I–1077*.

McGovern, P. J., and J. K. Morgan (2009), Volcanic spreading and lateral variations in the structure of Olympus Mons, Mars, *Geology*, *37*, 139–142, doi:10.1130/G25180A.1.

Mège, D., and P. Masson (1996), Amounts of stretching in Valles Marineris, *Planet. Space Sci.*, *44*, 749–782, doi:10.1016/0032-0633(96)00013-X.

Mitra, G., and A. J. Sussman (1997), Structural evolution of connecting splay duplexes and their implications for critical taper: An example based on geometry and kinematics of the Canyon Range culmination, Sevier Belt, central Utah, *J. Struct. Geol.*, *19*, 503–521, doi:10.1016/S0191-8141(96)00108-3.

Montgomery, D. R., S. M. Som, M. P. A. Jackson, B. C. Schreiber, A. R. Gillespie, and J. B. Adams (2009), Continental-scale salt tectonics on Mars and the origin of Valles Marineris and associated outflow channels, *Geol. Soc. Am. Bull.*, *121*, 117–133, doi:10.1130/B26307.1.

Moore, J. C., and R. von Huene (1980), Abnormal pore pressure and hole instability in forearc regions: A preliminary report, report, 29 pp., Oceans Margin Drill. Proj., Menlo Park, Calif.

Morgan, J. K., and P. J. McGovern (2005), Discrete element simulations of gravitational volcanic deformation: 2. Mechanical analysis, *J. Geophys. Res.*, *110*, B05403, doi:10.1029/2004JB003253.

Mount, V. S. (1989), State of stress in California and a seismic structural analysis of the Perdido Fold Belt, northwest Gulf of Mexico, Ph.D. dissertation, Princeton Univ., Princeton, N. J.

Mount, V. S., J. Suppe, and S. C. Hook (1990), A forward modeling strategy for balancing cross sections, *AAPG Bull.*, *74*, 521–531.

Mustard, J. F., et al. (2008), Hydrated silicate minerals on Mars observed by the Mars Reconnaissance Orbiter CRISM instrument, *Nature*, *454*, 305–309, doi:10.1038/nature07097.

Nemčok, M., S. Schamel, and R. Gayer (2005), *Thrustbelts: Structural Architecture, Thermal Regimes, and Petroleum Systems*, 554 pp., Cambridge Univ. Press, Cambridge, U. K.

Ohta, Y., and C. Akiba (Eds.) (1973), *Geology of the Nepal Himalayas*, 286 pp., Himalayan Committee of Hokkaido Univ., Saporro, Japan.

Okubo, C. H., and R. A. Schultz (2003), Thrust fault vergence on Mars: A foundation for investigating global-scale Tharsis-driven tectonics, *Geophys. Res. Lett.*, *30*(22), 2154, doi:10.1029/2003GL018664.

Okubo, C. H., and R. A. Schultz (2004), Mechanical stratigraphy in the western equatorial region of Mars based on thrust fault-related fold topography and implications for near-surface volatile reservoirs, *Geol. Soc. Am. Bull.*, *116*, 594–605, doi:10.1130/B25361.1.

Paterson, M. S., and T.-f. Wong (2005), *Experimental Rock Deformation–The Brittle Field*, 2nd ed., 348 pp., Springer, New York.

Phillips, R. J., et al. (2001), Ancient geodynamics and global-scale hydrology on Mars, *Science*, *291*, 2587–2591, doi:10.1126/science.1058701.

Plescia, J. B., and R. S. Saunders (1982), Tectonic history of the Tharsis region, Mars, *J. Geophys. Res.*, *87*, 9775–9791, doi:10.1029/JB087iB12p09775.

Plescia, J. B., L. E. Roth, and R. S. Saunders (1980), Tectonic features of southeast Tharsis, in *Reports of Planetary Geology Program*, *NASA Tech. Memo*. 81776, 68–70.

Price, N. J., and J. W. Cosgrove (1990), *Analysis of Geological Structures*, 520 pp., Cambridge Univ. Press, Cambridge, U. K.

Pruis, M. J., and K. L. Tanaka (1995), The Martian northern plains did not result from plate tectonics, *Lunar Planet. Sci.*, *XXVI*, Abstract 1147.

Saunders, R. S., L. E. Roth, G. S. Downs, and G. Schubert (1980), Early volcanic-tectonic province: Coprates region of Mars, in *Reports of Planetary Geology Program*, *NASA Tech. Memo*. 81776, 74–75.

Schofield, J. T., J. R. Barnes, D. Crisp, R. M. Haberle, S. Larsen, J. A. Magalhães, J. R. Murphy, A. Seiff, and G. Wilson (1997), The Mars Pathfinder Atmospheric Structure Investigation/Meteorology (ASI/MET) experiment, *Science*, *278*, 1752–1757, doi:10.1126/science.278.5344.1752.

Schultz, R. A. (1991), Structural development of Coprates Chasma and western Ophir Planum, central Valles Marineris rift, Mars, *J. Geophys. Res.*, *96*, 22,777–22,792.

Schultz, R. A. (1998), Multiple-process origin of Valles Marineris basins and troughs, Mars, *Planet. Space Sci.*, *46*, 827–834, doi:10.1016/S0032-0633(98)00030-0.

Schultz, R. A., and K. L. Tanaka (1994), Lithospheric-scale buckling and thrust structures on Mars: The Coprates rise and south Tharsis ridge belt, *J. Geophys. Res.*, *99*, 8371–8385, doi:10.1029/94JE00277.

Scott, D. H., and K. L. Tanaka (1986), Geologic map of the western equatorial region of Mars (1:15,000,000), *U.S. Geol. Surv. Misc. Inv. Ser. Map, I–1082-A*.

Seeber, L., J. G. Armbruster, and R. C. Quittmeyer (1981), Seismicity and continental subduction in the Himalayan arc, in *Zagros-Hindu Kush-Himalaya Geodynamic Evolution*, *Geodyn. Ser*, vol. 3, edited by H. K. Gupta and F. M. Delany, pp. 215–242, AGU, Washington, D. C.

Seely, D. R., P. R. Vail, and G. G. Walton (1974), Trench slope model, in *The Geology of Continental Margins*, edited by C. A. Burk and C. L. Drake, pp. 249–260, Springer, New York.

Sleep, N. H. (1994), Martian plate tectonics, *J. Geophys. Res.*, *99*, 5639–5655, doi:10.1029/94JE00216.

Snavely, P. D., Jr., H. C. Wagner, and D. L. Lander (1980), Geologic cross section of the central Oregon continental margin, *Geol. Soc. Am. Map Chart Ser., MC-28J.*

Solomon, S. C., and J. Chaiken (1976), Thermal expansion and thermal stress in the Moon and terrestrial planets: Clues to early thermal history, *Proc. Lunar Sci. Conf.*, *7th*, 3229–3243.

Solomon, S. C., et al. (2005), New perspectives on ancient Mars, *Science*, *307*, 1214–1220, doi:10.1126/science.1101812.

Suppe, J. (1980), Imbricated structure of western foothills belt, south-central Taiwan, *Pet. Geol. Taiwan*, *17*, 1–16.

Suppe, J. (1981), Mechanics of mountain building and metamorphism in Taiwan, *Geol. Soc. China Mem.*, *4*, 67–89.

Suppe, J. (2007), Absolute fault and crustal strength from wedge tapers, *Geology*, *35*, 1127–1130, doi:10.1130/G24053A.1.

Suppe, J., and C. Connors (1992), Critical taper wedge mechanics of fold-and-thrust belts on Venus: Initial results from Magellan, *J. Geophys. Res.*, *97*, 13,545–13,561, doi:10.1029/92JE01164.

Tanaka, K. L., and P. A. Davis (1988), Tectonic history of the Syria Planum province of Mars, *J. Geophys. Res.*, *93*, 14,893–14,917, doi:10.1029/JB093iB12p14893.

Tanaka, K. L., M. P. Golombek, and W. B. Banerdt (1991), Reconciliation of stress and structural histories of the Tharsis region of Mars, *J. Geophys. Res.*, *96*, 15,617–15,633, doi:10.1029/91JE01194.

Tanaka, K. L., J. M. Dohm, and T. R. Watters (1996), Possible coronae structures in the Tharsis region of Mars, *Lunar Planet. Sci.*, *XXVII*, Abstract 1315.

Thomson, B., and J. Head III (2001), Utopia Basin, Mars: Characterization of topography and morphology and assessment of the origin and evolution of basin internal structure, *J. Geophys. Res.*, *106*, 23,209–23,230, doi:10.1029/2000JE001355.

Toda, S., R. S. Stein, K. Richards-Dinger, and S. Bozkurt (2005), Forecasting the evolution of seismicity in southern California: Animations built on earthquake stress transfer, *J. Geophys. Res.*, *110*, B05S16, doi:10.1029/2004JB003415.

von Huene, R., G. W. Moore, and J. C. Moore (1979), Cross section of Alaska Peninsula-Kodiak Island-Aleutian Trench, *Geol. Soc. Am. Map Chart Ser., MC-28A*.

Watters, T. R. (1993), Compressional tectonism on Mars, *J. Geophys. Res.*, *98*, 17,049–17,060, doi:10.1029/93JE01138.

Watters, T. R. (2003), Lithospheric flexure and the origin of the dichotomy boundary on Mars, *Geology*, *31*, 271–274, doi:10.1130/0091-7613(2003)031<0271:LFATOO>2.0.CO;2.

Watters, T. R., and T. A. Maxwell (1986), Orientation, relative age, and extent of the Tharsis Plateau ridge system, *J. Geophys. Res.*, *91*, 8113–8125, doi:10.1029/JB091iB08p08113.

Watters, T. R., and P. J. McGovern (2006), Lithospheric flexure and the evolution of the dichotomy boundary on Mars, *Geophys. Res. Lett.*, *33*, L08S05, doi:10.1029/2005GL024325.

Watters, T. R., P. J. McGovern, and R. P. Irwin III (2007), Hemispheres apart: The crustal dichotomy boundary on Mars, *Annu. Rev. Earth Planet. Sci.*, *35*, 621–652, doi:10.1146/annurev.earth.35.031306.140220.

Webb, B. M. and J. W. Head (2002), Noachian tectonics of Syria Planum and the Thaumasia Plateau, *Lunar Planet. Sci.*, *XXXIII*, Abstract 1358.

White, R. S., and D. A. Ross (1979), Tectonics of the western Gulf of Oman, *J. Geophys. Res.*, *84*, 3479–3489, doi:10.1029/JB084iB07p03479.

Williams, C. A., C. Connors, F. A. Dahlen, E. J. Price, and J. Suppe (1994), Effect of the brittle-ductile transition on the topography of compressive mountain belts on Earth and Venus, *J. Geophys. Res.*, *99*, 19,947–19,974, doi:10.1029/94JB01407.

Williams, J.-P., F. Nimmo, W. B. Moore, and D. A. Paige (2008), The formation of Tharsis on Mars: What the line-of-sight gravity is telling us, *J. Geophys. Res.*, *113*, E10011, doi:10.1029/2007JE003050.

Wise, D. U., M. P. Golombek, and G. E. McGill (1979), Tharsis province of Mars: Geologic sequence, geometry, and a deformation mechanism, *Icarus*, *38*, 456–471, doi:10.1016/0019-1035(79)90200-8.

Worrall, D. M., and S. Snelson (1989), Evolution of the northern Gulf of Mexico, with emphasis on Cenozoic growth faulting and the role of salt, in *The Geology of North America: An Overview*, edited by A. W. Bally, pp. 97–137, Geol. Soc. of Am., Boulder, Colo.

Zuber, M. T., et al. (2000), Internal structure and early thermal evolution of Mars from Mars Global Surveyor topography and gravity, *Science*, *287*, 1788–1793, doi:10.1126/science.287.5459.1788.

A. L. Nahm, Center for Lunar Science and Exploration, USRA Lunar and Planetary Institute, 3600 Bay Area Blvd., Houston, TX 77058, USA. (nahma@mines.unr.edu)

R. A. Schultz, Geomechanics-Rock Fracture Group, Department of Geological Sciences and Engineering, University of Nevada, MS 172, Reno, NV 89557, USA.